Wireless Networks 9, 495–507, 2003

Performance Analysis of the Advanced Infrared (AIr) CSMA/CA MAC Protocol for Wireless LANs

V. VITSAS
Department of Informatics, Technological Educational Institution of Thessaloniki P.O. Box 14561, 54101 Thessaloniki, Greece

A.C. BOUCOUVALAS *
Multimedia Communications Research Group, School of Design, Engineering and Computing, Bournemouth University, Fern Barrow, Poole, Dorset, BH12 5BB, UK

Abstract. Advanced Infrared (AIr) is a proposed standard of the Infrared Data Association (IrDA) for indoor infrared LANs. AIr Medium Access Control (MAC) employs Carrier Sense Multiple Access with Collision Avoidance (CSMA/CA) techniques with Request To Send/Clear To Send (RTS/CTS) frame exchange to address the hidden station problem. A long Collision Avoidance Slot (CAS) duration, that includes the beginning of the CTS frame, is defined to cope with collisions caused from hidden stations. AIr MAC employs linear adjustment of the Contention Window (CW) size to minimize delays emerging from the long CAS duration. This paper provides a simple and accurate analytical model for the linear CW adjustment that calculates AIr throughput assuming a finite number of stations and error free channel transmissions. Validity of the model is verified by comparing analysis with simulation results. By examining the first derivative of the throughput equation, we derive the optimum CW size that maximizes throughput as a function of the network size. In the case of the AIr protocol, where a collision lasts exactly one CAS, different conclusions result for maximum throughput as compared with the corresponding conclusions for the similar IEEE 802.11 protocol. Using the proposed model, we present an extensive AIr throughput performance evaluation. The effectiveness of physical and link layer parameters on throughput performance is explored. The proposed long CAS duration combined with CW linear adjustment are proven quite effective. Linear CW adjustment combined with the long CAS duration offer an efficient collision avoidance scheme that does not suffer from collisions caused from hidden stations.

Keywords: IrDA, CSMA/CA, wireless LANs, optical wireless, performance evaluation

1. Introduction

Infrared Data Association (IrDA) was established in 1993 by major IT companies to develop standards for indoor, wireless connectivity using the unregulated infrared spectrum. The success of the IrDA 1.x platform architecture can be measured by the number of mobile devices on market today embedding IrDA ports. Over 40 million new devices are manufactured every year employing infrared ports for their wireless communication needs [22]. Device range includes laptop computers, digital cameras, mobile phones, printers, etc. The IrDA 1.x protocol supports half duplex, indoor, low cost, directed point to point links at a maximum distance of 1 m, an angle of ± 15 degrees at data rates up to 16 Mbit/s [8,14,22].

IrDA recently developed a new proposed standard called Advance Infrared (AIr) which allows a pool of users to share the infrared medium using a wide angle line of sight transmission model [15,22]. IrLAP, the IrDA 1.x data link layer [9], was split into three sub-layers, the AIr Medium Access Control (AIr-MAC) [11], the AIr Link Manager (AIr-LM) [12] and the AIr Link Control (AIr-LC) sub-layers. AIr MAC sub-layer is responsible for co-ordinating the access to the infrared medium among multiple AIr and IrDA 1.x devices. AIr LM is responsible for multiplexing multiple different client protocols and provides several priority and coexistence services. AIr LC layer is responsible for supporting connections to multiple devices. A new physical layer, AIr PHY [10], is proposed that uses a four-slot Pulse Position Modulation with Variable Repetition Encoding (4PPM/VR) format with a base data rate of 4 Mbps. Transmission rate varies from 250 Kbit/s to 4 Mbit/s, trading speed for range. Long-range AIr transceivers provide an effective range of 3.8 m at 4 Mbit/s and an effective range greater than 7.6 m at 250 Kbit/s [10]. Wide angle infrared AIr devices operate at an angle of ± 60 degrees. Physical layer issues for achieving the AIr MAC requirement for channel symmetry are discussed in [5,7] and AIr physical characteristics with experimental results can be found in [6]. An evaluation of the L-PPM encoding in infrared links employing repetition rate is presented in [18].

AIr MAC employs Carrier Sense Multiple Access with Collision Avoidance (CSMA/CA) techniques for medium access. AIr MAC provides Reliable and Unreliable transfer modes and Reserved media access by using the Request To Send/Clear To Send (RTS/CTS) frame exchange. A long Collision Avoidance Slot time (σ), which includes the beginning of the CTS frame is defined. A station contending for the medium first selects a random number z from range $(0, W-1)$, where W is Contention Window (CW). The station waits for z Collision Avoidance Slots (CAS) before transmitting in order to minimise the collision probability. AIr MAC also provides guidelines for linear CW adjustment. For

* Corresponding author.

the AIr protocol, linear CW adjustment is preferable than the exponential backoff of the similar IEEE 802.11 protocol because the AIr long CAS duration, combined with the high number of empty CAS introduced by the exponential backoff scheme, would result in significant delays. Throughput performance of AIr MAC's Unreserved transfer mode is presented in [21] by using simulation techniques. Performance evaluation of Reserved transfer modes by simulation is examined in [1,2,20]. Comparison of reserved modes by assuming an average delay due to the collision avoidance part of the protocol is presented in [17,19] and fair access of the infrared medium by all contending stations is considered in [16]. This work considers the collision avoidance procedures of the AIr protocol and provides an analytical model for the throughput performance of the AIr in the assumption of error free transmissions and finite number of stations. The key approximation in our model is the assumption of constant and independent collision probability of an RTS frame transmission regardless of the number of collisions the transmitting station has previously suffered. An analytical model based on the same assumption for the exponential CW backoff of the 802.11 protocol is presented in [3,4]. As proven by comparing analytical with simulation results, our model provides extremely accurate results for AIr throughput performance. Our model is employed to determine the effectiveness of physical and link layer parameters on throughput performance.

This paper is outlined as follows. Section 2 describes the AIr-MAC protocol, AIr's different transmission schemes and focuses on the collision avoidance procedures of the protocol. Section 3 defines saturation throughput and discusses implementation issues of AIr protocol. Section 4 develops an analytical model for AIr MAC throughput performance and section 5 validates the proposed model by comparing analysis and simulation results. Section 6 presents an analytical performance evaluation of AIr protocol, derives optimum CW size values for maximum throughput by differentiating the throughput equation and explores the effectiveness of physical and link layer parameters and delays to throughput performance. Concluding remarks are given in section 7.

2. Description of AIr-MAC protocol

The AIr MAC employs the Repetition Rates (*RR*) presented in table 1 [11]. The receiver monitors channel quality and advises the transmitter to implement a suitable *RR*. The transmitter repeats the symbols it transmits *RR* times to increase the symbol capture probability at the receiver. *RR* coding is very suitable for Pulse Position Modulation (PPM), which is used in AIr protocol. Doubling *RR* achieves a 3 dB SNR gain at the receiver for the same frame error rate [7,18]. A higher *RR* is also used to reach a station that is far away from the transmitter, thus trading speed for range.

Table 1
AIr RR enumeration.

Repetition rate	Data rate
$RR = 1$	4 Mbit/s
$RR = 2$	2 Mbit/s
$RR = 4$	1 Mbit/s
$RR = 8$	500 Kbit/s
$RR = 16$	250 Kbit/s

The AIr frame format is presented in figure 1. The Preamble (PA) field is transmitted for carrier sensing, symbol clock synchronisation and chip clock phase acquisition by the phase locked loop (PLL). The PA field is used by the receiver to lock on to and to detect the beginning of an incoming frame. The Synchronisation (SYNC) field enables exact identification of the start of the robust header field and qualifies the carrier detection based on the received PA. The Robust Header (RH) field contains the essential information required by the AIr PHY and AIr MAC layers to co-ordinate medium access. It is always transmitted using the maximum Repetition Rate encoding ($RR = 16$) to ensure that all stations in range receive this vital information. The Main Body (MB) field contains upper layer payload data and non-essential AIr MAC control information. MB may also contain MAC generated frame sequence numbers. When the MB field is present, it is followed by a Cyclic Redundancy Check (CRC) field protecting both the RH and MB fields.

The AIr MAC provides reliable and unreliable data transfer and reservation media access by employing the RTS/CTS frame exchange. Unreliable modes (figures 2(a), (b)) guarantee the transmission of user data but not the delivery as no acknowledgement is provided to indicate correct frame reception. Reliable modes guarantee correct frame reception as an acknowledgement is provided for every data packet (figure 2(c)) or for a packet burst (figure 2(d)). Reserved mode sequenced transfer (figure 2(d)) utilises the optional sequence number field of the MB frame portion to sequence transmitted frames. In reservation media access schemes (figures 2(a), (c), (d)), the transmitting station reserves the medium for the duration contained in the Reservation Time (RT) field of the RTS frame it transmits. The receiving station responds with a CTS frame and echoes the reservation period in the RT field of the CTS frame. As the RT field is contained in RH, it is

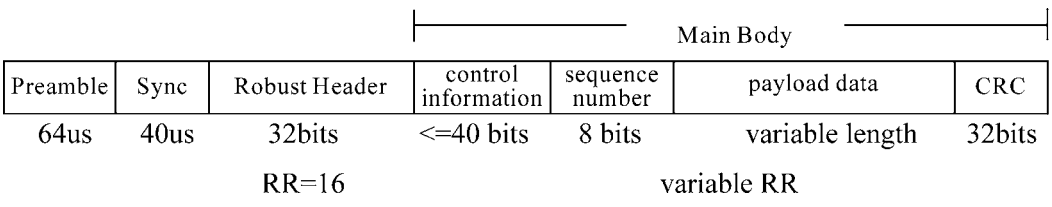

Figure 1. AIr frame format.

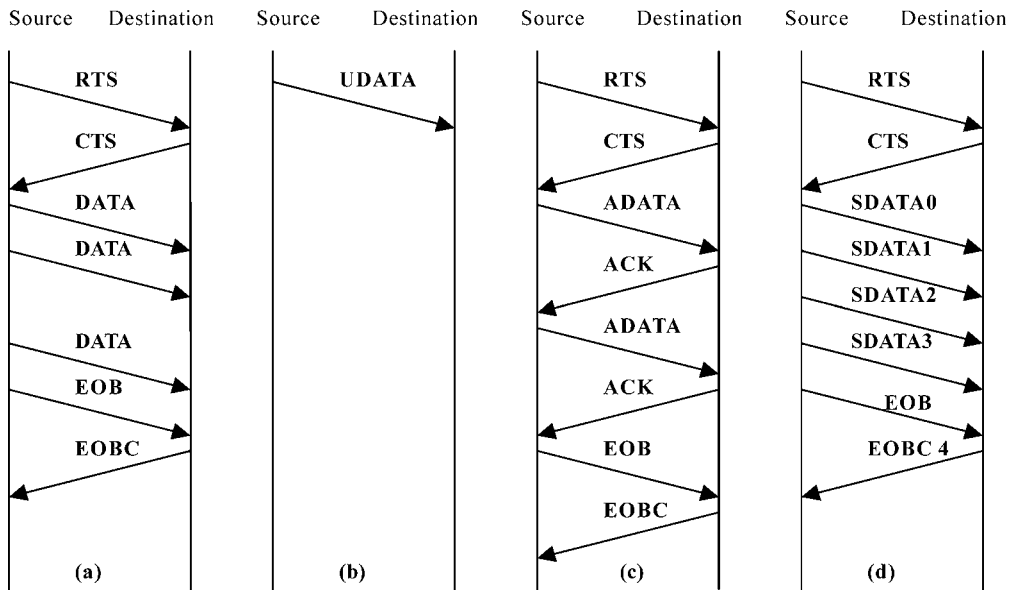

Figure 2. AIr transfer modes. (a) Reserved mode transfer with no acknowledgement (DATA frame); (b) Unreserved mode transfer (UDATA frame); (c) Reserved mode transfer with frame acknowledgement (ADATA frame); (d) Reserved mode Sequenced transfer (SDATA frame).

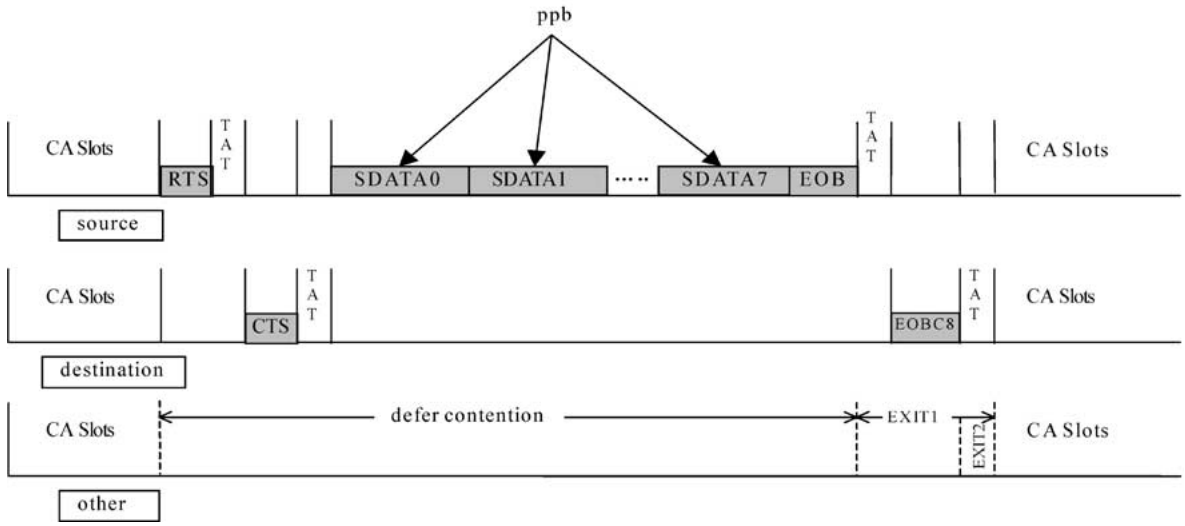

Figure 3. Reserved access scheme with sequenced mode transfer (SDATA frames).

always transmitted using maximum $RR = 16$ to ensure maximum coverage. Stations receiving only the RTS or only the CTS frame refrain from transmitting for the entire reservation period. RTS/CTS exchange is employed to address the hidden station problem [13], which occurs when two stations are unable to hear each other. When the transmitter receives the CTS frame, it initiates user data transmission. After the last data frame is transmitted and before the reservation time expires, the transmitter requests termination of current reservation by means of an End Of Burst (EOB) frame. The receiver confirms termination of current reservation by responding with an End Of Burst Confirm (EOBC) frame. Again stations hidden from the transmitting or from the receiving station realise that the current reservation is over by receiving the EOBC or the EOB frame, respectively.

The AIr MAC sub-layer is a Carrier Sense Multiple Access with Collision Avoidance (CSMA/CA) protocol [11]. The reserved mode sequenced transfer scheme presented in figure 2(d) is illustrated in figure 3. Stations with user data first contend for medium access. The contention period is slotted and a station is allowed to transmit only at the beginning of each slot time (σ). A station first selects a random number of CAS to defer transmission (this is the collision avoidance feature of the protocol) in order to minimise collision probability with other transmissions. This backoff number is uniformly selected in the range $(0, W - 1)$ and the backoff interval is assigned to CAS timer. W is the current CW and its value depends on the number of successful reservations and collisions experienced so far by the transmitting station. If during the deferral period another transmission is observed, the

CAS timer is freezed and restarted when the on-going reservation has finished and the next contention period has started. When the CAS timer reaches zero, the station transmits the RTS frame. While a transmitter is sending a frame, it blinds its own receiver such that it can not receive remote infrared pulses. The receiving station waits a minimum Turn Around Time (TAT) to allow for the transmitter's receive circuitry to recover and responds with a CTS frame. The transmitter, after a TAT delay, transmits user data and requests termination of current reservation by transmitting a EOB frame. AIr MAC pays significant care to synchronise all stations contending for the medium at exactly the same time after a reservation by employing a special synchronisation state on protocol's state transition diagrams. Synchronisation is accomplished by means of the EOB and EOBC frames indicating reservation termination as follows. All network stations (except from the receiver and from stations hidden from the transmitter) start the EXIT1 timer after receiving the EOB request as shown in figure 3. EXIT1 time duration is defined as the TAT after the EOB plus the transmission time of the EOBC frame plus the TAT after the EOBC frame. When a station's EXIT1 expires, the station contends for the medium by restarting the CAS timer. Thus, stations not hearing the EOBC frame contend for medium access at exactly the right time. Upon reception of the EOB frame, the receiver waits TAT and transmits the EOBC frame. This station and all stations that received the EOBC frame immediately start EXIT2 timer (and stop EXIT1 timer if it is active). EXIT2 is defined as the TAT delay (figure 3). When EXIT2 expires, the CAS timer is restarted and contention for medium access begins. This scheme ensures that, after a successful reservation, all stations (even stations hidden from the transmitter or from the receiver) are synchronised in contending for medium access at exactly the same time.

A contending station, after transmitting the RTS frame, starts the Wait For CTS (WFCTS) timer. If other (one or more) stations have selected the same CAS slot, they transmit their RTS frames at the same time. The collision is determined by the transmitting stations by the WFCTS timer expiration. The colliding stations select a new CAS slot and continue contending for medium access. To synchronise the colliding stations with the remaining stations, the WFCTS timer expires at the end of the current time slot.

The AIr Link Manager (LM) layer [12] is responsible for adjusting the CW size values. The adjustment algorithm should select "proper" CW values for the current network size and network load based on whether the station's previous reservation attempts were successful or not. Small CW values will result in a very high collision probability and large CW values will result in a large number of empty CAS slots. AIr LM specification [12] does not provide rules for CW adjustment but suggests guidelines for increasing and decreasing CW after one or more collisions and successful reservation attempts, respectively. AIr MAC defines CAS slot time (σ) as being greater than the transmission time of the RTS frame plus TAT plus the amount of time required to detect the beginning of the returning CTS frame ($T_{\mathrm{PA}} + T_{\mathrm{SYNC}}$). Such a long σ time ensures that even a contending station hidden from the transmitter but not from the receiver will not cause a collision unless, of course, it had selected the same CAS.

3. Saturation throughput performance and parameter definitions

In this work, we concentrate on saturation throughput for a fixed number of stations n. In saturation conditions, every station always has a burst of frames ready for transmission. In other words, the transmission queue for every station is always non empty. This saturation throughput performance figure is defined as the maximum load the system can reach in stable conditions. We also assume ideal channel conditions meaning that a noncolliding frame is always received error free to all network stations except from stations hidden from the transmitter. This work considers throughput performance of the two AIr MAC reserved access reliable transfer modes (figures 2(c), (d)); these modes include the transmission of acknowledgements at the MAC layer. All stations always employ the same Reserved mode reliable transfer scheme. After a successful reservation attempt, a station transmits *packets per burst* (ppb) frames of fixed payload size of l bits at a fixed data rate of C bit/s. As we do not consider channel bit errors, a *RR* increase resulting in higher symbol capture probability at the receiver is not considered. The MB of all data frames is always transmitted using $RR = 1$ and the RH portion is transmitted in the protocol suggested *RR* value of 16.

Based on AIr LM guidelines, current work implements a linear CW adjustment; CW increases by 4 after a collision and CW decreases by 4 after a successful reservation. AIr LM specification also poses limits for CW values; a minimum limit of 8 slots ($CW_{\min} = 8$) and a maximum limit of 256 slots ($CW_{\max} = 256$). Time required for transmitting frames and frame elements is presented in table 2. Table 3 presents timer delay values suggested by the standard, timer value restrictions and the corresponding values used in our model. All protocol suggested values are closely followed with an exception of the Wait For CTS (WFCTS) timer value. The value that obeys protocol's restrictions and, at the same time, synchronises the transmitter with other stations for the next contention period is implemented. Our model also adjusts the CAS timer to the beginning of the next slot if a transmission is observed during a CAS. All stations hearing the RTS frame

Table 2
AIr frame and frame element transmission times for $C = 4$ Mbps.

Frame/frame element	Duration	Time (usec)
T_{PA} (*frame element*)		64
T_{SYNC} (*frame element*)		40
T_{RH} (*frame element*)		128
TT_{RH} (*frame*)	$T_{\mathrm{PA}} + T_{\mathrm{SYNC}} + T_{\mathrm{RH}}$	232
T_{RTS} (*frame*)	$TT_{\mathrm{RH}} + 48/C$	244
T_{CTS} (*frame*)	TT_{RH}	232
T_{EOB} (*frame*)	TT_{RH}	232
T_{EOBC} (*frame*)	TT_{RH}	232
T_{ACK} (*frame*)	TT_{RH}	232

Table 3
AIr timers and delays.

Timer/delay	Restriction	Suggested (usec)	Implemented (usec)
Turn Around Timer (*TAT*)		200	200
CAS duration (σ)	$> T_{\text{RTS}} + TAT + T_{\text{PA}} + T_{\text{SYNC}}$	800	800
WFCTS Timer	$\geqslant TAT + TT_{\text{RH}}$	632	556
EXIT1 Timer	$= TAT + T_{\text{EOBC}} + TAT$	632	632
EXIT2 Timer	$= TAT$	200	200

will freeze the CAS timer upon reception of the PA field of the RTS frame. Stations hidden from the transmitter will receive only the CTS frame and will freeze their CAS timers upon reception of the PA field of the CTS frame. As this time difference will result in lack of CAS synchronisation during the next contention period, all CAS timers are adjusted to the beginning of the next CAS.

4. Analytical model

The key assumption used in this model is that an RTS transmission always collides with probability p regardless of the CW value used to select the deferral period for the reservation attempt. Our analytical model is divided into two parts. The first part considers the behaviour of a single station to compute p and the stationary probability τ that a station transmits in a randomly chosen CAS for a network of n stations. This probability is independent of the reserved access scheme employed by the stations. Then, by examining the events that can occur in a randomly chosen CAS, throughput performance is expressed as a function of probability τ.

4.1. RTS transmission probability

In the saturation conditions considered, all stations always have a burst of frames ready for transmission after a successful reservation. Let $b(t)$ be the stochastic process that represents the backoff time counter for a specific station. Process $b(t)$ does not represent the remaining time before a transmission attempt but follows an integer time scale that represents the number of the remaining CAS before transmission. Time scale is also slotted; t and $t+1$ represent the beginning of two consecutive slot times. Every station increments t at the beginning of every CAS. This discrete time scale is not directly related to system time as a successful reservation may occur between two consecutive CAS. As explained earlier, when an incoming RTS frame is received, the CAS timer is freezed and restated again at the beginning of the CAS that follows the successful reservation. Thus, the time between two CAS decrements in the t scale may involve a successful reservation.

The backoff counter for every station depends on the collisions and on the successful reservation attempts experienced by the station in the past. As a result, process $b(t)$ is non-Markovian. We define for convenience $W = CW_{\min}$. Let m be the "maximum backoff stage" defined as $CW_{\max} = W + 4m$ and we adopt the notation

$$W_i = W + 4i, \quad i \in (0, m), \tag{1}$$

where i is defined as the "backoff stage". AIr standard specifies $CW_{\max} = 256$ and $m = 62$. Let $s(t)$ be the stochastic process representing the backoff stage $(0, \ldots, m)$ of the station at time t.

The key approximation of this model is that a frame transmission collides with the same probability p regardless of the CW size used for this transmission. Based on this assumption and as p is assumed to be constant, the bidimensional process $\{s(t), b(t)\}$ can be modelled by the discrete-time Markov chain presented in figure 4. Adopting the short notation $P\{i_1, k_1 | i_0, k_0\} = P\{s(t+1) = i_1, b(t+1) = k_1 | s(t) = i_0, b(t) = k_0\}$, the only nonnull one-step transition probabilities are:

$$\begin{aligned}
&P\{i, k | i, k+1\} = 1, \quad k \in (0, W_i - 2),\ i \in (0, m),\\
&P\{i, k | i+1, 0\} = \frac{1-p}{W_i},\\
&\quad k \in (0, W_i - 1),\ i \in (0, m-1),\\
&P\{i+1, k | i, 0\} = \frac{p}{W_{i+1}},\\
&\quad k \in (0, W_{i+1} - 1),\ i \in (0, m-1),\\
&P\{0, k | 0, 0\} = \frac{1-p}{W_0}, \quad k \in (0, W_0 - 1),\\
&P\{m, k | m, 0\} = \frac{p}{W_m}, \quad k \in (0, W_m - 1).
\end{aligned} \tag{2}$$

The first equation in (2) represents the fact that a station decrements the collision avoidance timer for the entire slot time period until it reaches zero. The second equation considers the fact that after a successful reservation attempt the CW is decreased and the new CAS value is uniformly chosen from the range $(0, W_i - 1)$. The third equation accounts for the fact that after an unsuccessful reservation attempt the CW is increased and the new CAS value is uniformly chosen from the larger range. The fourth equation considers the fact that after a successful reservation attempt at stage 0 the CW is not decreased and the fifth equation considers that after an unsuccessful reservation attempt at stage m the CW is not further increased.

Let $b_{i,k} = \lim_{t\to\infty} P\{s(t) = i, b(t) = k\},\ i \in (0, m),\ k \in (0, W_i - 1)$ be the stationary distribution of the chain.

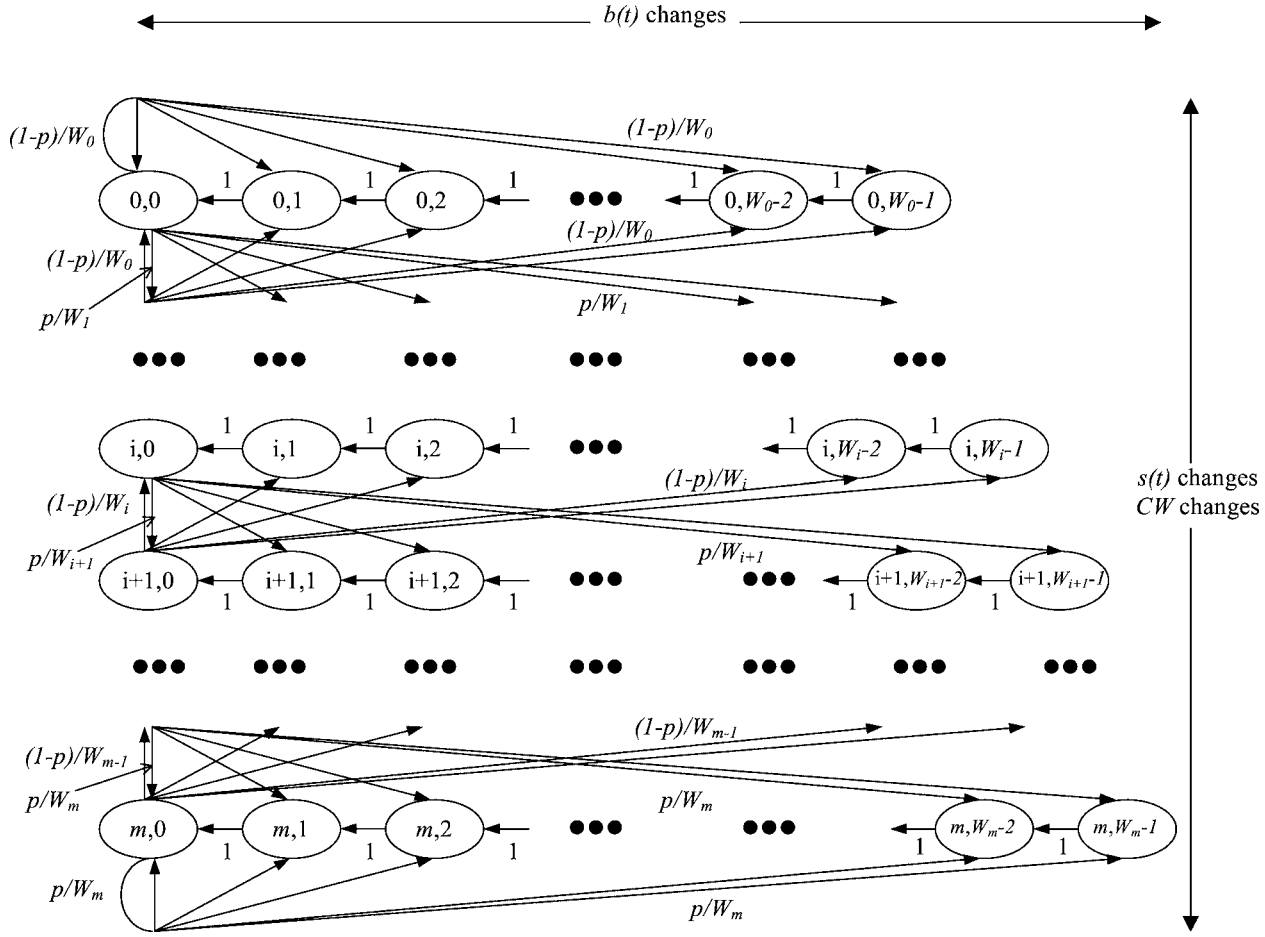

Figure 4. Markov Chain model for backoff CW.

Considering that $b_{00} = (1-p)b_{00} + (1-p)b_{10}$, b_{10} is given by

$$b_{10} = \frac{p}{1-p} b_{00}. \tag{3}$$

Taking into account that $b_{10} = pb_{00} + (1-p)b_{20}$, b_{20} is given by

$$b_{20} = \left(\frac{p}{1-p}\right)^2 b_{00}. \tag{4}$$

Using the same method, it can be easily shown that

$$b_{i0} = \left(\frac{p}{1-p}\right)^i b_{00}, \quad i \in (0, m). \tag{5}$$

Owing to chain regularities, for each $k \in (0, W_i - 1)$,

$$\begin{aligned} b_{0k} &= \frac{W_0 - k}{W_0}\big(b_{10}(1-p) + b_{00}(1-p)\big), \\ b_{ik} &= \frac{W_i - k}{W_i}\big(b_{i+1,0}(1-p) + b_{i-1,0}p\big), \\ &\quad i \in (1, m-1), \\ b_{mk} &= \frac{W_m - k}{W_m}(b_{m-1,0}p + b_{m0}p). \end{aligned} \tag{6}$$

After some algebra

$$\begin{aligned} b_{0k} &= \frac{W_0 - k}{W_0} b_{00}, \\ b_{ik} &= \frac{W_i - k}{W_i} b_{i0}, \quad i \in (1, m-1), \\ b_{mk} &= \frac{W_m - k}{W_m} b_{m0}. \end{aligned} \tag{7}$$

Equations (7) can be rewritten as

$$b_{ik} = \frac{W_i - k}{W_i} b_{i0}, \quad i \in (0, m),\ k \in (0, W_i - 1). \tag{8}$$

Equations (5) and (8) express all $b_{i,k}$ values as a function of b_{00} and of probability p. To find b_{00} the normalisation condition can be applied

$$\begin{aligned} 1 &= \sum_{i=0}^{m} \sum_{k=0}^{W_i - 1} b_{ik} \\ &= \sum_{i=0}^{m} b_{i0} \sum_{k=0}^{W_i - 1} \frac{W_i - k}{W_i} = \sum_{i=0}^{m} b_{i0} \frac{W_i + 1}{2} \\ &= \frac{b_{00}}{2} \sum_{i=0}^{m} \left(\frac{p}{1-p}\right)^i (W_i + 1) \end{aligned} \tag{9}$$

and by considering equation (1)

$$1 = \frac{b_{00}}{2}\left[(W+1)\sum_{i=0}^{m}\left(\frac{p}{1-p}\right)^i + 4\sum_{i=0}^{m} i\left(\frac{p}{1-p}\right)^i\right]. \quad (10)$$

After some algebra

$$1 = \frac{b_{00}}{2}\left[(W+1)\frac{(1-p)^{m+1}-p^{m+1}}{(1-2p)(1-p)^m} + \frac{4p(1-p)}{(1-2p)^2} \times \left(1 - \frac{p^m(1+m)-p^{m+1}(2m+1)}{(1-p)^{m+1}}\right)\right]. \quad (11)$$

Equation (11) expresses b_{00} as a function of the conditional collision probability p, the smallest implemented contention window size W and the number of employed backoff stages m. Using the above analysis, the probability τ that a station transmits in a randomly chosen slot time can be evaluated. As a station transmits when the backoff timer reaches the value of zero,

$$\tau = \sum_{i=0}^{m} b_{i0} = b_{00}\sum_{i=0}^{m}\frac{p^i}{(1-p)^i} = b_{00}\frac{(1-p)^{m+1}-p^{m+1}}{(1-2p)(1-p)^m}. \quad (12)$$

Substituting the value of b_{00} from equation (11) to equation (12), τ is given by

$$\tau(p) := \tau = \frac{2}{(W+1) + \frac{4p((1-p)^{m+1}+(2m+1)p^{m+1}-(m+1)p^m)}{((1-p)^{m+1}-p^{m+1})(1-2p)}}. \quad (13)$$

Probability τ depends on collision probability p which is still unknown. The probability p that a reservation attempt collides is the probability that at least one of the remaining $n-1$ stations transmit in the same slot time. Assuming that all stations "see" the discrete-time Markov chain presented in figure 4 in the steady state and transmit with probability τ in a randomly chosen slot time,

$$p = 1 - (1-\tau)^{n-1}. \quad (14)$$

Equations (13) and (14) form a nonlinear system in the unknowns τ and p. The system can be solved by employing numerical methods evaluating τ and p for a certain W and m combination. It is easy to prove that there is a unique solution to the nonlinear system. Equation (14) can be rewritten as:

$$\tau^*(p) := \tau = 1 - (1-p)^{1/(n-1)}. \quad (15)$$

The function $\tau^*(p)$ is a continuous and monotone increasing function in the range $p \in (0, 1)$. It increases from $\tau^*(0) = 0$ to $\tau^*(1) = 1$. Function $\tau(p)$ is a continuous and monotone decreasing function in the same range. It decreases from $\tau(0) = 2/(W+1)$ to $\tau(1) = 2/(W+1+4m)$. Continuity in correspondence of the critical value $p = 1/2$ is proven by considering that in this case equation (5) reduces to $b_{i0} = b_{00},\ i \in (0, m)$, and equation (9) becomes

$$1 = \frac{b_{00}}{2}\sum_{i=0}^{m}(W_i+1) = \frac{b_{00}}{2}\sum_{i=0}^{m}(W+4i+1) = \frac{b_{00}}{2}\left((m+1)(W+1)+4\sum_{i=0}^{m} i\right) \quad (16)$$

and b_{00} is given by $b_{00} = 2/((m+1)(W+2m+1))$. In this case $\tau(1/2) = (m+1)b_{00} = 2/(W+2m+1)$. Uniqueness of the solution is proven by considering that $\tau(0) > \tau^*(0)$ and $\tau(1) < \tau^*(1)$.

4.2. Throughput analysis

Based on the station transmission probability τ and on the RTS collision probability p evaluated in the previous section, throughput efficiency can be evaluated. P_{tr} is defined as the probability that at least one reservation attempt occurs in a given slot time. For a network of n stations, each transmitting with probability τ, P_{tr} is given by

$$P_{\text{tr}} = 1 - (1-\tau)^n. \quad (17)$$

The probability P_{s} that an occurring RTS transmission is successful is given by the probability that one station transmits and the remaining $n-1$ stations remain silent provided that at least one transmission occurs in the channel:

$$P_{\text{s}} = \frac{n\tau(1-\tau)^{n-1}}{1-(1-\tau)^n}. \quad (18)$$

A successful transmission in a randomly selected slot occurs with probability $P_{\text{tr}}P_{\text{s}}$ and the time transmitting payload information is given by $P_{\text{s}}P_{\text{tr}}lppb/C$. The average slot duration can be evaluated by considering that with probability $1 - P_{\text{tr}}$ the slot is empty; with probability $P_{\text{tr}}P_{\text{s}}$ the slot contains a successful transmission and with probability $P_{\text{tr}}(1-P_{\text{s}})$ the slot contains a collision. Thus, throughput efficiency S can be evaluated by dividing the time transmitting payload information in a slot time with the average slot duration

$$S = \frac{P_{\text{tr}}P_{\text{s}}lppb/C}{(1-P_{\text{tr}})\sigma + P_{\text{tr}}P_{\text{s}}T_{\text{s}} + P_{\text{tr}}(1-P_{\text{s}})T_{\text{c}}}, \quad (19)$$

where T_{s} is the slot duration when a successful transmission occurs, T_{c} is the slot duration for a collision involving two or more simultaneous frame transmissions and σ is the CAS time duration. A collision always lasts exactly one CAS and therefore

$$T_{\text{c}} = \sigma. \quad (20)$$

Considering (20), throughput equation (19) can be easily reduced to

$$S = \frac{P_{\text{tr}}P_{\text{s}}lppb/C}{P_{\text{tr}}P_{\text{s}}T_{\text{s}} + \sigma - P_{\text{tr}}P_{\text{s}}\sigma}. \quad (21)$$

For AIr networks employing the Reserved transfer mode with frame acknowledgements (ADATA frame) (figure 2(c)):

$$T_S^{\text{ADATA}} = T_{\text{RTS}} + TAT + T_{\text{CTS}} + TAT + \left(T_{\text{PA}} + T_{\text{SYNC}} + T_{\text{RH}} + \frac{l+72}{C} + TAT + T_{\text{ACK}} + TAT\right)ppb + T_{\text{EOB}} + TAT + T_{\text{EOBC}} + TAT. \quad (22)$$

Finally, if the Reserved transfer mode with sequenced data (SDATA frame) (figure 2(d)) is used:

$$T_S^{\text{SDATA}} = T_{\text{RTS}} + TAT + T_{\text{CTS}} + TAT + \left(T_{\text{PA}} + T_{\text{SYNC}} + T_{\text{RH}} + \frac{l+80}{C}\right)ppb + T_{\text{EOB}} + TAT + T_{\text{EOBC}} + TAT. \quad (23)$$

Current analysis allows evaluation of all component tasks affecting the AIr throughput. Such an evaluation reveals the main factors resulting in throughput degradation for AIr performance when unsuitable values for physical and link layer parameters are selected. The amount of time that the channel is idle because no station transmits during a CAS slot is

$$S_{\text{empty}} = \frac{(1-P_{\text{tr}})\sigma}{P_{\text{tr}}P_{\text{s}}T_{\text{s}} + \sigma - P_{\text{tr}}P_{\text{s}}\sigma}. \quad (24)$$

Time portion used on collisions caused by simultaneous transmissions by two or more stations is

$$S_{\text{coll}} = \frac{P_{\text{tr}}(1-P_{\text{s}})\sigma}{P_{\text{tr}}P_{\text{s}}T_{\text{s}} + \sigma - P_{\text{tr}}P_{\text{s}}\sigma}. \quad (25)$$

Time portion taken on transmitting data frame overheads and on transmitting the RTS/CTS and EOB/EOBC frames during a successful reservation period is given by

$$S_{\text{over}} = \frac{P_{\text{tr}}P_{\text{s}}(T_{\text{s}} - lppb/C)}{P_{\text{tr}}P_{\text{s}}T_{\text{s}} + \sigma - P_{\text{tr}}P_{\text{s}}\sigma}. \quad (26)$$

5. Model validation

The analytical model presented in the previous section is validated by comparing its results with that obtained using the AIr simulator developed in [20]. The AIr simulator is developed using the OPNET modeler from MIL3 Inc. and infrared transmissions are emulated by altering the radio version of the OPNET modeler. The simulator emulates the real operation of a station as closely as possible, by implementing the collision avoidance procedures and all parameters such as frame transmission times and turn around times. The AIr MAC finite state machine is implemented and user written C/C++ code is executed when entering and/or exiting each state.

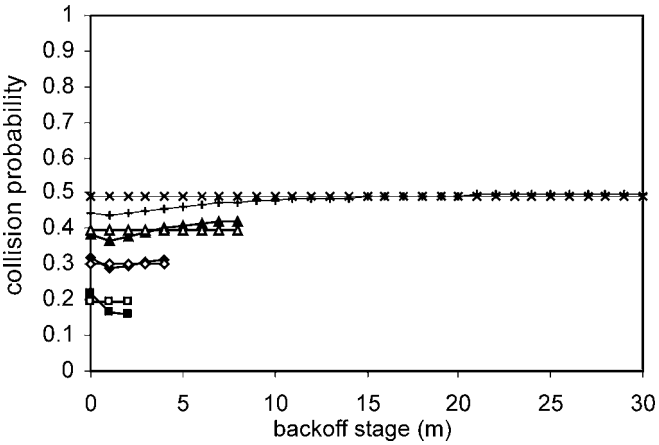

Figure 5. Collision probabilities: analysis versus simulation, $W = 8$, $m = 62$, SDATA frames, $l = 16$ Kbits, $ppb = 8$, $C = 4$ Mbit/s. □: $n = 2$, analysis; ◇: $n = 3$, analysis; △: $n = 5$, analysis; ×: $n = 30$, analysis; ■: $n = 2$, simulation; ♦: $n = 3$, simulation; ▲: $n = 5$, simulation; +: $n = 30$, simulation.

We first focus on the behaviour of a single station. The probability that a station's transmission is at stage i is denoted by q_i. The analytical model calculates q_i probabilities by

$$q_i = \frac{b_{i0}}{\tau}, \quad i = 0, 1, \ldots, m. \quad (27)$$

Probability p_i is defined as the collision probability of a station's transmission at stage i. The key assumption of the analytical model can now be expressed as

$$p = p_i = constant, \quad i = 0, 1, \ldots, m. \quad (28)$$

Figure 5 compares simulation (p_i) and analysis (p) probabilities for the proposed values for the W and m parameters. Simulation results are acquired with a 95% confidence interval lower than 0.007. Figure includes only stages with transmission probability q_i higher than 0.01 and shows that high back off stages are rarely used in small networks. Slight differences are noticed between the simulation p_i probabilities and the p value that the analytical model uses to approximate them. Noticeable differences at low stages for large networks ($n = 30$) are not significant as the transmission probability (q_i) of low stages significantly lowers when networks size increases. Figure 5 validates the intuitive understanding that the key assumption of the analytical model is more accurate when n increases; only for $n = 2$ noticeable differences between p_i and p are observed at low stages that simultaneously have high transmission probabilities q_i. In addition, simulation results indicate that the collision probability p_i is not significantly different at high stages, as it might have been expected.

Figure 6 shows that the analytical model is extremely accurate for calculating AIr performance. Analytical results (lines) match with simulation results (symbols) for different W, m and ppb values. Figure 6 also shows that the differences observed in figure 5 between p and p_i probabilities for $n = 2$ have minimal effect on the ability of the analytical model to precisely estimate throughput performance. Simulation re-

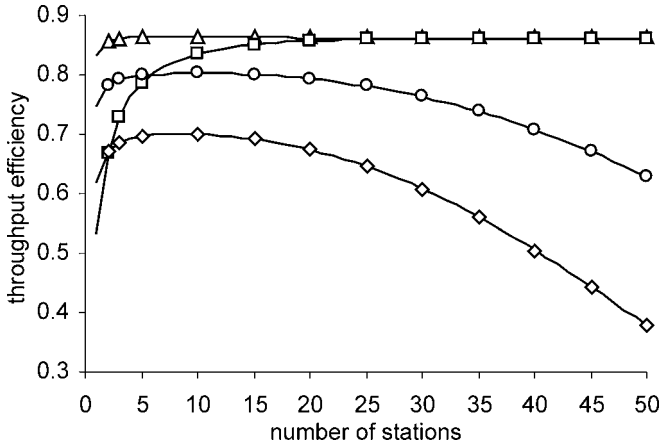

Figure 6. Saturation throughput: analysis versus simulation, SDATA frames, $l = 16$ Kbits, $C = 4$ Mbit/s. △: $W = 8$, $m = 62$, $ppb = 8$; □: $W = 64$, $m = 62$, $ppb = 8$; ◇: $W = 8$, $m = 4$, $ppb = 2$; ○: $W = 8$, $m = 5$, $ppb = 4$.

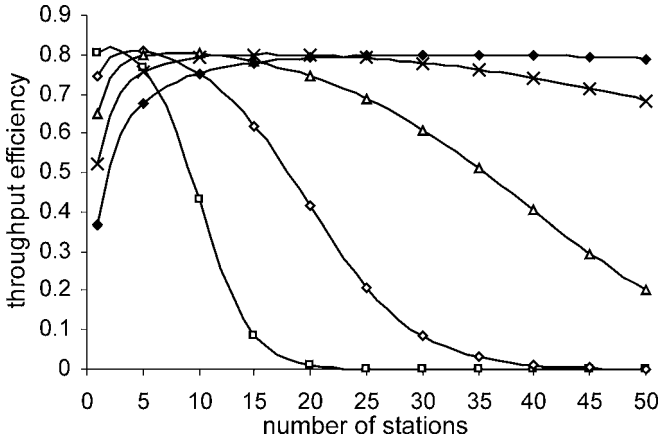

Figure 7. Throughput efficiency versus n for fixed CW size, SDATA frames, $l = 16$ Kbits, $ppb = 4$, $C = 4$ Mbit/s. □: $CW(slots) = 4$; ◇: $CW(slots) = 8$; △: $CW(slots) = 16$; ×: $CW(slots) = 32$; ♦: $CW(slots) = 64$.

sults are obtained with a 95% confidence interval lower than 0.003.

6. Performance evaluation

The effectiveness of the proposed CW size adjustment is explored first. Figure 7 plots throughput efficiency versus number of stations for various fixed CW size values, i.e., no CW size adjustment is enforced after a successful reservation or collision. Results are produced by employing current analysis for $m = 0$. Throughput results for $n = 1$ are also included in figure 7 because n refers to the number of transmitting stations in a network scenario and not to the number of stations participating in the network. Figure 7 shows that throughput efficiency degrades for small network scenarios, especially when a large CW size is implemented. When n increases throughput efficiency reaches a maximum value. The n value resulting in maximum throughput increases when the implemented CW size value is increased. Further network size increase results in significant throughput degradation, especially for small CW size values. As a conclusion, a proper CW size value should be selected for a given network size for maximum throughput.

Figure 8 shows all factors affecting throughput versus network size for fixed $CW = 16$. For small numbers of stations, as related to the implemented CW size value, the increased number of CAS empty slots decreases throughput performance. When n increases empty slot significance is eliminated resulting in high throughput but for large number of users the increased number of collisions results in poor performance. Maximum throughput is observed when a suitable CW for the network size is used that results in a very small number of collisions and empty CAS simultaneously.

Optimum CW (W_{opt}) value for a LAN with n transmitting stations can be evaluated by employing the proposed analytical model for $m = 0$ and by setting the first derivative of the throughput equation versus τ equal to zero. When $m = 0$, the model's key assumption that a transmission collides with the same probability regardless of the CW value used to select the deferral period is always true because CW is fixed in this case. By rearranging equation (21)

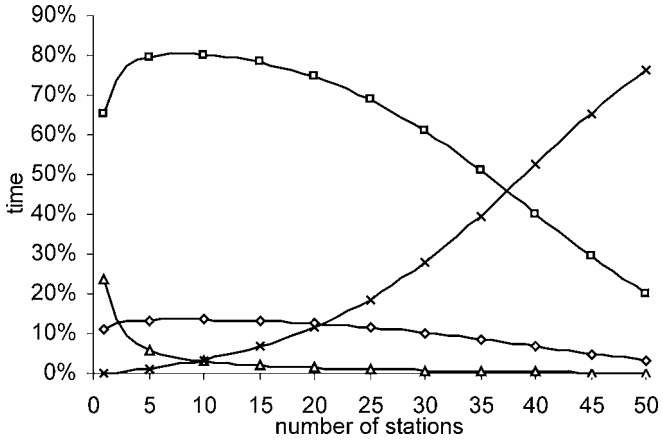

Figure 8. Time allocation of various AIr tasks versus n for fixed CW size = 16 slots, SDATA frames, $l = 16$ Kbits, $ppb = 4$, $C = 4$ Mbit/s. □: useful data transmission (throughput efficiency); ◇: transmitting SDATA frame overheads and RTS/CTS/EOB/EOBC control frames; △: empty CAS; ×: collisions.

$$S = \frac{lppb/C}{T_{\text{s}} - \sigma + \sigma/(P_{\text{tr}}P_{\text{s}})}. \tag{29}$$

Considering that l, ppb, C, T_{s} and σ are constants, throughput is maximized when the expression

$$u = P_{\text{tr}}P_{\text{s}} \tag{30}$$

is maximized. By substituting P_{tr} and P_{s} values from equations (17) and (18), equation (30) becomes

$$u = n\tau(1-\tau)^{n-1}. \tag{31}$$

By taking the first derivative of equation (31) versus τ and setting it equal to zero, after some algebra we obtain

$$\tau_{\text{opt}} = \frac{1}{n}. \tag{32}$$

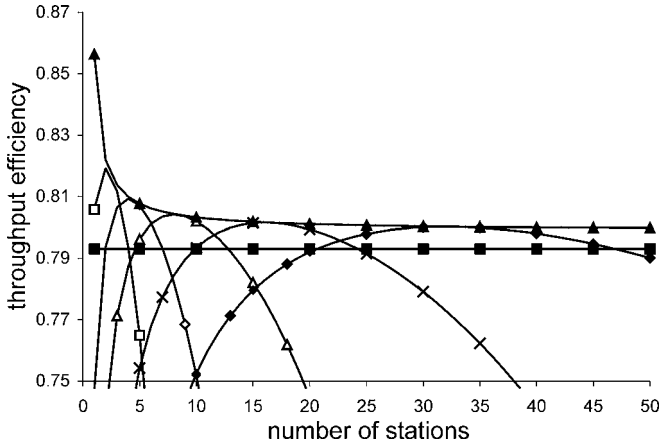

Figure 9. Throughput efficiency versus n for fixed CW size, SDATA frames, $l = 16$ Kbits, $ppb = 4$, $C = 4$ Mbit/s. □: $CW(slots) = 4$; ◇: $CW(slots) = 8$; △: $CW(slots) = 16$; ×: $CW(slots) = 32$; ♦: $CW(slots) = 64$; ▲: maximum $S_{\max}$; ■: maximum S_{appr}.

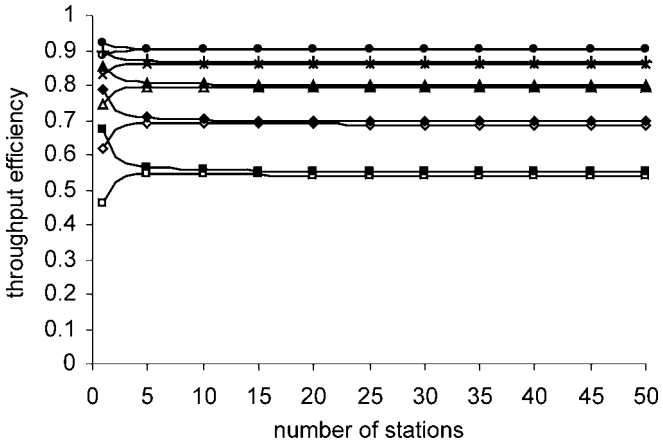

Figure 10. Throughput efficiency versus n, SDATA frames, $l = 16$ Kbits, $W = 8$, $m = 62$, $C = 4$ Mbit/s. □: $ppb = 1$; ◇: $ppb = 2$; △: $ppb = 4$; ×: $ppb = 8$; ○: $ppb = 16$; ■: $ppb = 1$, $S_{\max}$; ♦: $ppb = 2$, $S_{\max}$; ▲: $ppb = 4$, $S_{\max}$; +: $ppb = 8$, $S_{\max}$; •: $ppb = 16$, $S_{\max}$.

To reach optimum transmission probability τ_{opt} stations should employ the optimum CW size W_{opt}. When $m = 0$, equation (13) reduces to

$$\tau = \frac{2}{W+1}. \tag{33}$$

Combining equations (32) and (33)

$$W_{\text{opt}} = 2n - 1. \tag{34}$$

Maximum throughput can be evaluated from equation (29) if we substitute P_{tr} and P_{s} from equations (17) and (18) for τ_{opt} given from equation (32)

$$S_{\max} = \frac{lppb/C}{T_{\text{s}} - \sigma + \sigma(n/(n-1))^{n-1}}. \tag{35}$$

As a result, maximum throughput depends on the number of transmitting stations in the LAN. However, for large n maximum throughput reaches a steady value. This conclusion is slightly different with the expressed conclusion in [4] that maximum throughput is independent of n for the exponential backoff adjustment scheme of the IEEE 802.11 protocol although linear and exponential backoff schemes coincide when no adjustment ($m = 0$) is allowed. Different conclusions arise from the approximations necessary for calculating maximum throughput in [4] because [4] considers the general case where a collision lasts several CAS time periods, as in the 802.11 protocol. Figure 9 plots throughput efficiency versus number of stations for fixed CW values and focuses on the maximum achievable throughput (note that the y-axis ranges from 0.75 to 0.87). It also plots $S_{\max}$ given from equation (35) and the approximated maximum throughput S_{appr} calculated by performing the approximations presented in [4] for AIr's physical and link layer parameter values. The figure shows that when collisions last exactly one CAS duration, as in the AIr protocol, the approximations proposed in [4] result in a lower calculated maximum throughput performance.

The effectiveness of the AIr CW size adjustment scheme is explored in figure 10, which compares $S_{\max}$ with AIr throughput efficiency (S) versus network size for different *ppb* values. The proposed adjustment algorithm is proved quite effective as AIr throughput is very close to maximum for $n > 5$; significant differences are observed only for small networks. Figure 10 also shows that throughput efficiency increases when the number of frames transmitted during a successful reservation (*ppb* parameter) increases. AIr practically relies on large *ppb* values for efficient performance as it reaches very poor operation when only 16 Kbits ($ppb = 1$) of user data are transmitted during a successful reservation. As applications may often transmit even fewer data across a local area network, AIr is not efficient for such network scenarios.

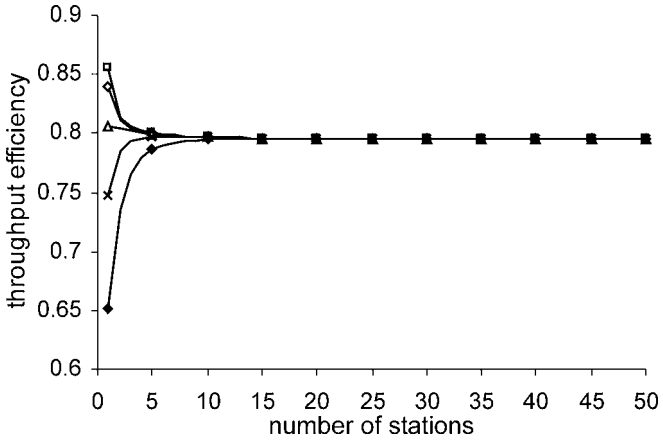

Figure 11. Throughput efficiency versus n, SDATA frames, $m = 62$, $l = 16$ Kbits, $ppb = 4$, $C = 4$ Mbit/s. □: $W = 1$; ◇: $W = 2$; △: $W = 4$; ×: $W = 8$; ♦: $W = 16$.

Figure 10 also suggests that maximum performance is not achieved when only a few stations are competing for medium access. For such small networks, the minimum CW size value of 8 is significantly larger than the optimum CW value given by (34). As a result, the large number of empty CAS causes significant throughput degradation. Figure 11 plots throughput efficiency versus network size for different W ($W = CW_{\min}$) values. It reveals that for large networks,

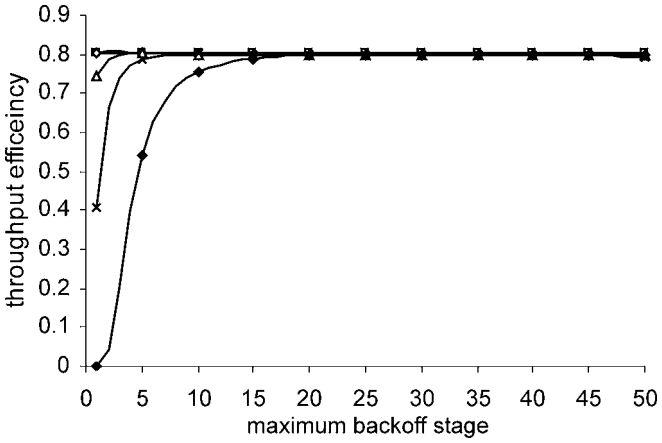

Figure 12. Throughput efficiency versus maximum backoff stage m, SDATA frames, $W = 4$, $l = 16$ Kbits, $ppb = 4$, $C = 4$ Mbit/s. □: $n = 1$; ◊: $n = 5$; △: $n = 10$; ×: $n = 20$; ♦: $n = 50$.

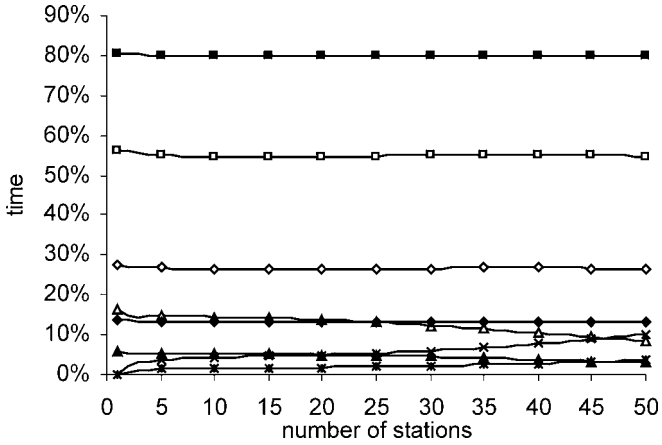

Figure 13. Time allocation of various AIr tasks versus n, SDATA frames, $W = 4$, $m = 20$, $l = 16$ Kbits, $C = 4$ Mbit/s. □: useful data transmission (throughput efficiency), $ppb = 1$; ◊: transmitting overheads, $ppb = 1$; △: empty slots, $ppb = 1$; ×: collisions, $ppb = 1$; ■: useful data transmission (throughput efficiency), $ppb = 4$; ♦: transmitting overheads, $ppb = 4$; ▲: empty slots, $ppb = 4$; ✳: collisions, $ppb = 4$.

throughput performance is independent from the initial CW size value. However, for small networks a throughput increase is observed as W gets smaller. If only one station transmits in the LAN, maximum throughput is observed for $W = 1$. This value coincides with the W_{opt} value given by (34) for $n = 1$ and actually disables the collision avoidance (CA) scheme, which delays medium access if only one station transmits in the LAN. However, simulation results indicate that using $W = 1$ leads to channel capture by one station for $n > 1$. A fairness problem is observed for $W = 2$ and $W = 3$, where all stations do not get an equal chance in accessing the medium. The fairness problem is eliminated when W is greater or equal to 4. Thus, for the considered network scenarios, W should be safely reduced to four in order to increase throughput for small networks. Figure 12 presents the suitability of CW_{max} value selected in the standard by plotting throughput efficiency versus m values for different network sizes for $W = 4$, $l = 16$ Kbits and $ppb = 4$. It shows that throughput is not practically affected as long as m is greater than 20. This m value yields a value for CW_{max} of 64, which is significantly smaller than the proposed value of 256. These results can be explained as follows. For a specific network size, linear adjustment directs the average CW values implemented by competing stations close to the optimal CW size given by equation (34). As a result, for small networks ($n < 5$), the proposed CW_{min} value of 8 should be lowered in order to allow stations to implement CW sizes close to the optimum value. Because the proposed CW_{max} value of 256 is suitable for a larger than normal number of contending stations ($n = 128$, equation (34)), CW_{max} can be safely lowered. The proposed CW_{max} value of 64 is significantly smaller than the W_{opt} value equation (34) calculates for $n = 50$ because throughput performance is not very sensitive to the average CW value for large networks. Comparing current conclusions for CW_{min} and CW_{max} values for the AIr linear CW adjustment with results presented in [4] for the IEEE 802.11 exponential CW adjustment, we can conclude that much smaller values should be used in the linear as compared to the exponential adjustment. A station implementing the 802.11 exponential backoff uses CW_{min} after every successful reservation attempt. As a result, the proper selection of CW_{min} becomes of key importance for the performance of the exponential backoff scheme and a relatively large CW_{min} should be employed to avoid collisions. In addition, exponential backoff should implement a large CW_{max} value to minimise the collision probability after a small number of successive collisions. In the linear approach, as CW_{min} is used only after a large number of successful reservation attempts, CW_{min} can be safely lowered even for large network sizes. As the CW is increased by a small number (by 4) after a collision, large CW_{max} values are not often reached. As a conclusion, low CW_{min} and CW_{max} values can be implemented in linear CW adjustment.

Figure 13 plots all time consuming tasks versus network size for different ppb values to demonstrate the factors resulting in throughput impairment for small ppb values. It reveals that the time portions utilized in empty slots and in collisions are always minimal and that the main factor that reduces throughput is always the time portion utilized on transmitting overheads during a successful reservation, i.e., transmitting SDATA frame headers and control (RTS/CTS/EOB/EOBC) frames. The reason is that in order to ensure maximum coverage, the RH is always transmitted using $RR = 16$. As a result, to cope with potential hidden nodes, applications must transmit large amounts of data in every successful reservation. If the Reserved mode with Acknowledgement (ADATA frames) is used, further throughput degradation, caused by the additional Acknowledgement frames, is shown in figure 14. Figure 15 plots throughput efficiency versus network size for $C = 250$ Kbps for different ppb values and SDATA frame employment. At this data rate, AIr employs $RR = 16$ in transmitting payload data. As a result, the RH field and payload data are transmitted using the same RR. A significant throughput efficiency increase is observed and large ppb values are no longer a necessity in or-

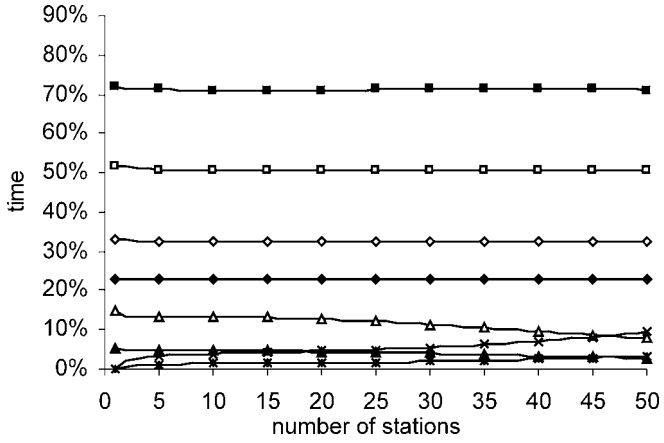

Figure 14. Time allocation of various AIr tasks versus n, ADATA frames, $W = 4$, $m = 20$, $l = 16$ Kbits, $C = 4$ Mbit/s. □: useful data transmission (throughput efficiency), $ppb = 1$; ◊: transmitting overheads, $ppb = 1$; △: empty slots, $ppb = 1$; ×: collisions, $ppb = 1$; ■: useful data transmission (throughput efficiency), $ppb = 4$; ♦: transmitting overheads, $ppb = 4$; ▲: empty slots, $ppb = 4$; ✳: collisions, $ppb = 4$.

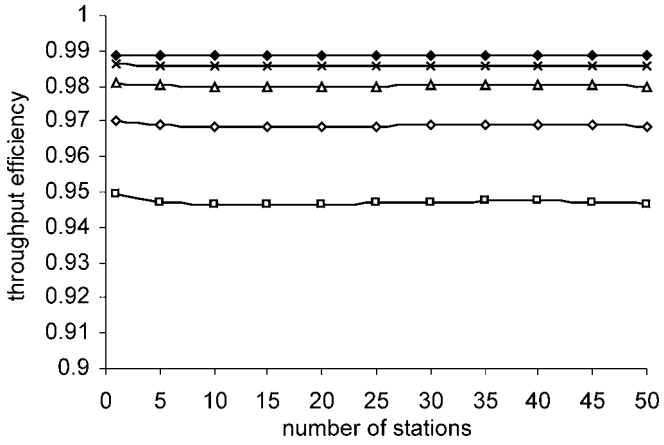

Figure 15. Throughput efficiency versus n, SDATA frames, $W = 4$, $m = 20$, $l = 16$ Kbits, $C = 250$ Kbit/s ($RR = 16$). □: $ppb = 1$; ◊: $ppb = 2$; △: $ppb = 4$; ×: $ppb = 8$; ♦: $ppb = 16$.

der to obtain excellent throughput efficiency (note that the y-axis ranges from 0.9 to 1.0). As a conclusion, AIr's large ppb value requirement for high throughput is caused by the high RR used in transmitting the RH portion of frames; the large CAS time period (σ) and the CW adjustment algorithm implemented do not result in significant throughput degradation.

Figure 16 explores the effectiveness of transmitting the RH field of all frames using $RR = 1$ and of reducing the minimum turn around time for applications transmitting only 16 Kbits of data ($ppb = 1$) during every successful reservation. A significant throughput efficiency increase is observed if the RH field is transmitted using $RR = 1$. Figure 16 also shows the throughput efficiency increase obtained by reducing the minimum turnaround time (TAT), a physical layer parameter. For all these cases, a smaller CAS slot time should be implemented, always obeying the restriction that $\sigma \geqslant T_{\text{RTS}} + TAT + T_{\text{PA}} + T_{\text{SYNC}}$ as it must ensure that a station not hearing the RTS frame will hear the beginning of the

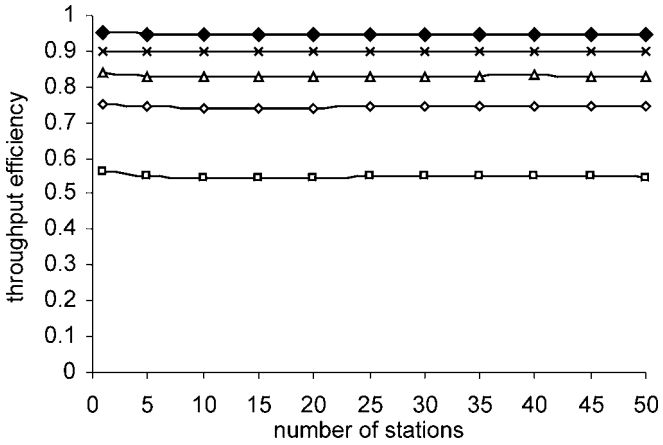

Figure 16. Throughput efficiency versus n, SDATA frames, $W = 4$, $m = 20$, $l = 16$ Kbits, $ppb = 1$, $C = 4$ Mbit/s. □: RH field in $RR = 16$, $TAT = 200$ us; ◊: RH field in $RR = 1$, $TAT = 200$ us; △: RH field in $RR = 1$, $TAT = 100$ us; ×: RH field in $RR = 1$, $TAT = 50$ us; ♦: RH field in $RR = 1$, $TAT = 10$ us.

Table 4
AIr physical and link layer parameters for improved performance.

Parameter	$RR = 16$	$RR = 1$	$RR = 1$	$RR = 1$	$RR = 1$
TAT	200	200	100	50	10
$T_{\text{RTS}} + TAT + T_{\text{PA}} + T_{\text{SYNC}}$	548	233	133	83	43
CAS duration (σ)	800	300	200	100	50

CTS frame during the CAS time duration. The values used are displayed in table 4.

7. Conclusions

This paper presents an analytical model to compute AIr throughput performance assuming finite number of stations and error free transmissions. Comparison with simulation results confirms that the model predicts AIr throughput performance accurately. The model is employed to evaluate throughput efficiency for various network scenarios. Results indicate that the proposed large Collision Avoidance Slot duration combined with the linear Contention Window adjustment are quite effective in achieving excellent throughput performance. Considering that this scheme also deals with collisions caused by hidden stations, it provides an efficient choice for Collision Avoidance procedures.

AIr throughput results indicate that the high Repetition Rate ($RR = 16$) used to transmit the Robust Header of AIr frames results in significant throughput degradation, especially when small amounts of data are transmitted in every successful reservation. The problem can be addressed by transmitting a number of data frames during every successful reservation or by reducing the RR employed in transmitting the RH field or by reducing the minimum turnaround time, a physical layer parameter.

References

[1] P. Barker and A.C. Boucouvalas, A simulation model of the Advanced Infrared (AIr) MAC protocol using OPNET, in: *Second International Symposium on Communication Systems Networks and Digital Signal Processing*, Bournemouth University, UK, July 18–20 (2000) pp. 153–156.

[2] P. Barker and A.C. Boucouvalas, Performance comparison of the IEEE 802.11 and AIr infrared wireless MAC protocols, in: *Proc. of the 2nd Annual Symposium on the Convergence of Telecommunications, Networking & Broadcasting*, Liverpool JMU, UK, June 18–19 (2001) pp. 113–118.

[3] G. Bianchi, IEEE 802.11: saturation throughput analysis, IEEE Communications Letters 2(12) (1998) 318–320.

[4] G. Bianchi, Performance analysis of the IEEE 802.11 distributed coordination function, JSAC Wireless Series 18(3) (2000).

[5] A.C. Boucouvalas and P. Barker, Asymmetry in optical wireless links, IEE Optoelectronics 147(4) (2000) 313–321.

[6] F. Gfeller and W. Hirt, A robust wireless infrared system with channel reciprocity, IEEE Communications Magazine 36(12) (1998) 100–106.

[7] F. Gfeller and W. Hirt, Advanced Infrared (AIr): Physical layer for reliable transmission and medium access, in: *Proceedings of 2000 International Zurich Seminar on Broadband Communications* (2000) pp. 77–84.

[8] D.J.T. Heatly, D.R.Wisely, I. Neild and P. Cochrane, Optical wireless: The story so far, IEEE Communications Magazine 36(12) (1998) 72–82.

[9] Infrared Data Association, Serial Infrared Link Access Protocol (IrLAP), Version 1.1 (IrDA, 1996).

[10] Infrared Data Association, Advanced Infrared Physical Layer Specification (AIr-PHY), Version 1.0 (IrDA, 1998).

[11] Infrared Data Association, Advanced Infrared (AIr) MAC Draft Protocol Specification, Version 1.0 (IrDA, 1999).

[12] Infrared Data Association, Advanced Infrared (AIr) Link Manager Draft Specification, Version 0.3 (IrDA, 1999).

[13] L. Kleinrock and F. Tobagi, Packet switching in radio channels, Part II – the hidden terminal problem in carrier sense multiple access and the busy tone solution, IEEE Transactions in Communications 23(12) (1975) 1417–1433.

[14] I. Millar, M. Beale, B.J. Donoghue, K.W. Lindstrom and S. Williams, The IrDA standard for high-speed infrared communications, The Hewlett-Packard Journal 49(1) (1998) 10–26.

[15] T. Ozugur, J.A. Copeland, M. Naghshineh and P. Kermani, Next generation indoor infrared-LANs: issues and approaches, IEEE Personal Communications Magazine (December 1999) 6–19.

[16] T. Ozugur, M. Naghshineh, P. Kermani and J.A. Copeland, Fair media access for wireless LANs, in: *Proc. of IEEE GLOBECOM'99*, Rio de Janeiro, Brasil (December 1999) pp. 570–579.

[17] T. Ozugur, M. Naghshineh, P. Kermani and J.A. Copeland, On the performance of ARQ protocols in infrared networks, International Journal of Communication Systems 13 (2000) 617–638.

[18] T. Ozugur, M. Naghshineh, P. Kermani, C.M. Olsen, B. Rezvani and J.A. Copeland, Performance evaluation of L-PPM links using repetition rate coding, in: *Proc. of IEEE PIMRC'98*, Boston, MA (September 1998) pp. 698–702.

[19] T. Ozugur, M. Naghshineh, P. Kermani, C.M. Olsen, B. Rezvani and J.A. Copeland, ARQ protocol for infrared wireless LANs: packet-level ACK or no-packet-level ACK?, in: *Proc. of IEEE ICUPC'98*, Florence, Italy (October 1998) pp. 1235–1239.

[20] V. Vitsas and A.C. Boucouvalas, Performance analysis of the AIr-MAC optical wireless protocol, in: *Proceedings of the International Conference on System Engineering, Communications and Information Technologies, (ICSECIT 2001)*, Department of Electrical Engineering, University of Magallanes, Punta Arenas, April 16–19, Chile (2001).

[21] V. Vitsas and A.C. Boucouvalas, Performance evaluation of IrDA advanced infrared AIr-MAC protocols, in: *Proceedings of the fifth Multi-Conference on Systemics, Cybernetics, and Informatics*, Vol. 4, Orlando, FL, July 22–25 (2001) pp. 347–352.

[22] S. Williams, IrDA: past, present and future, IEEE Personal Communications 7(1) (2000) 11–19.

Vasileios Vitsas received his B.Sc. degree in electrical engineering from University of Thessaloniki, Greece in 1983, his M.Sc. degree in computer science from University of California, Santa Barbara, in 1986 and his Ph.D. degree in wireless communications from Bournemouth University, UK in 2002. In 1988 he joined Hellenic Telecommunications Organisation where he worked in the field of X.25 packet switching networks. In 1994 he joined Technological Educational Institution of Thessaloniki, Greece as a lecturer in Computer Networks. His current research interests lie in wireless and multimedia communications. He is a member of the Technical Committee of IEEE Globecom 2002. Dr. Vitsas is a member of IEEE, Greek Computer Society and Technical Chamber of Greece.
E-mail: vitsas@it.teithe.gr

Anthony C. Boucouvalas graduated with a B.Sc. in electrical and electronic engineering from Newcastle upon Tyne University in 1978. He received his M.Sc. and D.I.C. degrees in communications engineering, in 1979, from Imperial College, where he also received his Ph.D. degree in fibre optics in 1982. Subsequently he joined GEC Hirst Research Centre, and became Group Leader and Divisional Chief Scientist working on fibre optic components, measurements and sensors, until 1987, when he joined Hewlett Packard Laboratories as Project Manager. At HP he worked in the areas of optical communication systems, optical networks, and instrumentation, until 1994, when he joined Bournemouth University. In 1996 he became a Professor in multimedia communications, and in 1999 he became Director of the Microelectronics and Multimedia Research Center. His current research interests lie in optical wireless communications, multimedia communications, and human–computer interfaces. He has published over 120 papers in the areas of fibre optics, optical fibre components, optical wireless communications and Internet Communications, and HCI. Professor Boucouvalas is a Fellow of IEEE, a Fellow of IEE, a Fellow of the Royal Society for the encouragement of Arts, Manufacturers and Commerce, (FRSA), a Member of the New York Academy of Sciences, and ACM. He is an editor of IEEE Transactions on Wireless Communications, an editor of IEEE Wireless Communications Magazine and Secretary of the IEEE UK&RI Communications Chapter. He is in the Organising Committee of the International Symposium on Communication Systems Networks and Digital Signal Processing, (CSNDSP), and a member of Technical Committees of numerous conferences, including IEEE Globecom and ICC.
E-mail: tboucouv@bournemouth.ac.uk
WWW: http://dec.bournemouth.ac.uk/staff/tboucouvalas/tony1.htm